

Performance comparison of TOPAS chirped fiber Bragg grating sensor with Tanh and Gaussian apodization

Dedi Irawan¹, Khaikal Ramadhan², Saktioto², Azwir Marwin²

¹Optoelectronics Laboratory Physics, Department of Physics Education, FMIPA, Universitas Riau, Pekanbaru, Riau, Indonesia

²Plasma and Photonics Laboratory, Department of Physics, FMIPA, Universitas Riau, Pekanbaru, Riau, Indonesia

Article Info

Article history:

Received Jan 10, 2022

Revised Apr 19, 2022

Accepted Apr 21, 2022

Keywords:

Apodization

Chirped fiber Bragg grating

Gaussian

Tanh

Temperature Sensor

TOPAS

ABSTRACT

In this work we carried out a numerical simulation with software Optigrating for Apodization chirped fiber Bragg grating (CFBG) with TOPAS material to improve sensitivity sensor, it was found that CFBG with a grating length of 50 mm has advantages in terms of ripple factor, side lobe left (SLL), and side lobe right (SLR) with values of -0,998 and -10,5264 dB, respectively. While the 10 mm CFBG has a narrower full-width half maximum (FWHM) with a value of 0.4528 nm. Tanh and Gaussian apodization were arranged in the CFBG design, it was found that the Tanh linear-CFBG had a narrow FWHM but for the ripple factor and the main lobe and side lobes were not good enough compared to the Tanh Cubicroot-CFBG, and the same pattern was also obtained in the Gaussian apodization. The narrow FWHM indicates the accuracy in detecting temperature, as well as the suppression of SLL and SLR. for the effect of apodization on CFBG it was found that The Tanh Linear-CFBG design with TOPAS material has the highest sensitivity which is -51.76 pm/oC compared to other designs.

This is an open access article under the [CC BY-SA](https://creativecommons.org/licenses/by-sa/4.0/) license.



Corresponding Author:

Dedi Irawan

Department Physics Education, PMIPA, Universitas Riau

Pekanbaru, Riau, Indonesia

Email: dedi.irawan@lecturer.unri.ac.id

1. INTRODUCTION

Fiber Bragg grating (FBG) which has a grating with a periodically changing refractive index has received great attention in recent years, FBG can be used as optical filters, dispersion compensation in optical communications, and optical sensors [1]. The behavior of the Bragg grating which can filter the input signal makes it a widely preferred and researched wavelength-based sensor. Factors such as not being susceptible to electromagnetic waves, small size, fast and safe response, and biocompatibility make FBG attractive to researchers. This has happened since the demonstration of photon-induced refractive index modulation in the last three decades. FBG sensor grating has different shapes and is used in various fields such as the oil and gas industry [2], aviation [3], medical [4], strain sensing [5], and temperature [6], [7], and monitoring in nuclear plants [8]. In general, FBG is sensitive to changes in physical parameters such as strain and temperature independently, which we cannot separate the effects of the two quantities normally, but requires special measures, as well as simultaneous temperature and strain sensing. Physical information such as temperature and strain is encoded in terms of wavelengths. The wavelength of transmission and reflection of the reflected signal through the grating provides inseparable information on the influence of temperature and the effect of the strain. In separating the effects of the two solutions, the second FBG isolated from the strain is used as a reference in temperature measurements while a single FBG is left to measure the temperature and strain quantities [9], [10].

Several solutions have been given to separate the effects of strain and temperature, such as the use of FBG with different ion doping [11], slanted grating FBG, and interrogation. The method option is carried out with optical power to distinguish the effect of cross-sensitivity between temperature and strain, but this method provides disadvantages such as low interrogation speed due to the low optical spectrum detection speed, so an interrogation system is needed for simulated and real-time temperature and strain monitoring.

Photosensitivity exploitation has been carried out to enrich the FBG typology by creating a non-uniform grating shape. Such exploitation depends on the fiber characteristics and the modulating refractive index [12], as a result of this it will be possible to produce an apodization grating [1] that can reject the main spectrum lobe or the shifting grating. The variation of the refractive index modulation period makes it possible to obtain chirped fiber Bragg grating (CFBG) [13]. CFBG has a reflection spectrum that varies along the grating this happens because each part of the grating reflects a different spectrum. The configuration in CFBG makes the Bragg wavelength vary linearly along the grating axis so that CFBG has a greater reflectance spectrum than uniform FBG in full-width half maximum (FWHM). Uniform FBG has a length of up to 50 mm with sensing distance limited to 10 mm, while CFBG has a typical length of 15-50 mm so that it has the potential to distinguish spatial events that occur, with this capability CFBG can be an alternative in temperature and strain sensing [13], [14], monitoring damage to hybrid composites [15] and measuring shock and detonation velocity [16], [17].

In a paper, it was reported that CFBG was used in evaluating the sensitivity to temperature with the 3 nm band using the transfer matrix method in addition to evaluating the temperature, variations in the position, and width of the heating on the grating was also carried out [4]. Giovanna *et al.* [18] described the dependence of CFBG on grating parameters which were optimized for several applications and also used a wide bandwidth of 56 nm for thermo ablation medical applications. Most of the CFBG studies have only been carried out for linear gratings both in temperature sensor applications to demonstrate the gradient of the Bragg wavelength shift within a given temperature [19], temperature sensing for possible applications in biomedicine [18], and CFBG applications in optical communications such as dispersion compensation. In data transfer [20] reported studies for the analysis of the effect of apodization in dispersion compensation [21] and also used in WDM technology as a reflector for different apodizations [22], [23], as well as in dense wavelength-division multiplexing (DWDM) technology in overcoming pulse widening optical communication [24].

CFBG contained in single-mode fiber has been used in several applications, including the design of CFBG with a length of 50 mm as a temperature sensor and a chirping speed of 0.8 nm/mm, CFBG with a length of 15 mm and a chirping speed of 1.33 nm/mm, 45 mm long and chirping speed. 1.24nm/mm, and CFBG with a length of 45 mm and a chirp speed of 1.24 nm/mm, most CFBG only use silica which is more expensive than CFBG with polymer materials such as TOPAS, polymethyl methacrylate (PMMA), and Tera Flex. Meanwhile, the need for optical sensors to increase in many applications, so FBG with polymer materials can be an alternative in its use and improve their performance with apodizations [18], [19], [25], [26].

In this work, we improve perform of CFBG TOPAS material with Tanh and Gaussian apodization and then analyze its application as a temperature sensor, parameters such as grating length, profile apodization are analyzed as sensor applications. By using Optigrating. The analysis will be carried out for each spectrum produced, other types of CFBG such as quadratic, square root, and cubic root become the dominant part of this study [27].

2. THEORY

When the signal enters the CFBG, the signal will be filtered, part of the signal is reflected and some of it is forwarded. The reflected wavelength is called the Bragg wavelength, mathematically it can be shown in (1).

$$\lambda_{Bragg} = 2n_{eff}\Lambda \quad (1)$$

The effective refractive index along the fiber can be defined as in (2).

$$n_{eff}(z) = n_0 + f(z)\Delta n_{ac}v \cos\left(\left(\frac{2\pi}{\Lambda}\right)z + \theta(z)\right) \quad (2)$$

where z is the position, n_0 is FBG's initial refractive index, Λ grating period, Δn_{ac} modulation refractive index amplitude, $f(z)$ apodization function, is the chirp function where C is the chirp parameter, v fringe

visibility. $\theta(z) = 2\pi Cz^2/\Lambda$. the working scheme of CFBG can be seen in Figure 1, CFBG has a grating that is not the same distance but has regular differences, this factor will affect the wavelength produced, in general with a lattice structure like this it will give more ripples around the center of the long waves and also has a wider range of wavelengths than the uniform FBG, the transmission spectrum has ripples around the center of the wavelength, these ripples are usually used for optical communication to compensate for the dispersion that occurs along with the optical fiber, For optical sensors, the important thing and consider is how much the reflection spectrum shifts with changes in the environment, in this case changes in temperature to be clearer can be seen in Figure 1.

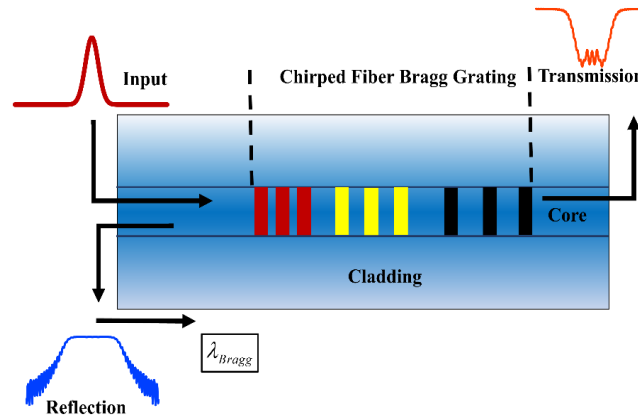


Figure 1. CFBG Scheme

The Bragg wavelength is affected by the distribution of the effective refractive index and the lattice period, as described in (1) and the effective refractive index of the FBG is influenced by the apodization profile and the type of chirping on the FBG grating, mathematically it can be seen in (2). Linear-CFBG mathematically the CFBG-linear grating structure can be seen in (3).

$$\Lambda(z) = \Lambda_0 - \frac{z-L/2}{L} \Delta \tag{3}$$

linear-CFBG has a linearly different distance between gratings, as seen in (3), the CFBG grating is arranged linearly along with the FBG core.

Quadratic-CFBG for quadratic-CFBG the distance between the grating structures in the core is defined as in (4).

$$\Lambda(z) = \Lambda_0 - \left[\left(\frac{z}{L} \right)^2 - \frac{1}{4} \right] \Delta \tag{4}$$

meanwhile, for quadratic-CFBG, the distance between the gratings corresponds to the quadratic function, the CFBG grating is arranged along with the core with the distance forming a quadratic function.

Squareroot-CFB: for square root-CFBG the distance between the grating structures in the core is defined as in the (5).

$$\Lambda(z) = \Lambda_0 - \left[\sqrt{\frac{z}{L}} - \frac{1}{\sqrt{2}} \right] \Delta \tag{5}$$

Squareroot-CFBG has a continuous grating in the core with the distance between the gratings equal to the square root function.

Cubicroot-CFBG and the last type is cubicroot-CFBG, the distance between the gratings in the FBG core is defined as in (6).

$$\Lambda(z) = \Lambda_0 - \left[\sqrt[3]{\frac{z}{L}} - \frac{1}{\sqrt[3]{2}} \right] \Delta \tag{6}$$

For cubicroot-CFBG has a lattice along the core which is arranged according to the cubic root function. Where $\Lambda(z)$ grating period, Λ_0 initial grating, period and Δ total chirp, L is grating length. In this work the effect of CFBG types on the resulting spectrum will be analyzed, meanwhile, the shift in the Bragg wavelength from the FBG can be seen mathematically in (7).

$$\Delta\lambda_b = \lambda_b(\alpha + \vartheta)\Delta T \quad (7)$$

From the equation we can see that the Bragg wavelength λ_b is affected by the wavelength λ_b , coefficient of thermal expansion α , thermo optical coefficient ϑ and changes in temperature ΔT .

3. METHOD

The method used in this research is to perform a numerical simulation of coupled-mode theory in explaining the behavior of the transmission and reflection spectra of CFBG, then it will be varied for grating lengths with different CFBG structures, the resulting lobes of each spectrum will be investigated. The CFBG parameter used is TOPAS with a refractive index of 1.53 and 1.525 in this work, we use Optigrating software to analyze the transmission and reflection spectrum of CFBG. The parameters of the CFBG design are in Table 1.

Table 1. CFBG parameters

Parameters	Value
Period	0.53219361
Grating Shape	sinus
Average index	uniform
Periode Chirp	Linear, quadratic, square root, and cubic root
Mod. Index	0.0001
Total Chirp	0.1 nm
Expansion thermal	$6 \times 10^{-5}/^{\circ}C$
Thermo-optic	$-9.3 \times 10^{-5}/^{\circ}C$
Grating length	10 mm, 20 mm, 30 mm, 40 mm, and 50 mm

After defining the parameters on the CFBG, the transmission spectrum and reflection spectrum will be obtained, in this case CFBG uses TOPAS polymer material with the coefficient of thermal expansion and thermo-optical coefficient as shown in the Table 1. After all defined will be shown the shift in the reflection wavelength or sensitivity of the CFBG design. The shift in the reflection wavelength is closely related to the sensitivity of the CFBG, in this case CFBG is used as a temperature sensor.

4. RESULTS AND DISCUSSION

In this work we use optigrating software to simulate and design a CFBG sensor, the parameters used in this simulation are FBG with TOPAS material with a refractive index of 1.53 for the core and 1.525 for the cladding. Further related to the parameters used can be seen in Table 1. FBG periodic grating will allow FBG to pass certain wavelengths, meanwhile, CFBG will provide wider spectrum, which will be advantageous in optical communication as dispersion compensation by delaying wavelength-dependent differential groups, we performed numerical simulation using coupled-mode theory In generating the transmission and reflection spectrum for each type of CFBG, in the following we will vary the length of the CFBG grating and will look at the position of side lobe left (SLL), side lobe right (SLR), FWHM and different main lobe and sidelobe and FWHM bandwidth, as shown in Figure 2. The reflection and transmission spectrum can be seen clearly in Figure 2(a) and Figure 2(b) respectively.

Coupled-mode theory (CMT) is used in analyzing the spectrum for any given grating length, several grating lengths have been applied in several fields, such as reported that FBG with a narrow FWHM is good for temperature and strain monitoring, in the world of optical communication as a dispersion compensator that FBG can pass wavelengths. After being simulated using CMT and CFBG linear type used in this analysis, the reflection signal is obtained for variations in grating length, CFBG with a grating length of 10 mm has an FWHM width of 0.4528, SLL at a position of 1549,7144 nm with a power of 0.4528. SLL is -13.7218 dB, meanwhile when viewed from the SLR it is at 1550.2856 nm with an SLR power of -13.7258 dB. The main-lobe peak is at a wavelength of 1550 nm. From these results, we can know the difference between SLL and SLR to the main-lobe of 0.2856 nm respectively. This data was obtained when the CFBG was designed at a temperature of 25 °C.

CFBG with a grating length of 20 mm has an FWHM width of 0.544 nm and SLL and SLR positions are at 1550.2704 nm and 1549.7296 nm respectively, while the peak spectrum is at a wavelength of 1550.044 so that it has a difference of 0.044 nm when compared to 10 mm CFBG. It can be seen in the Table 2.

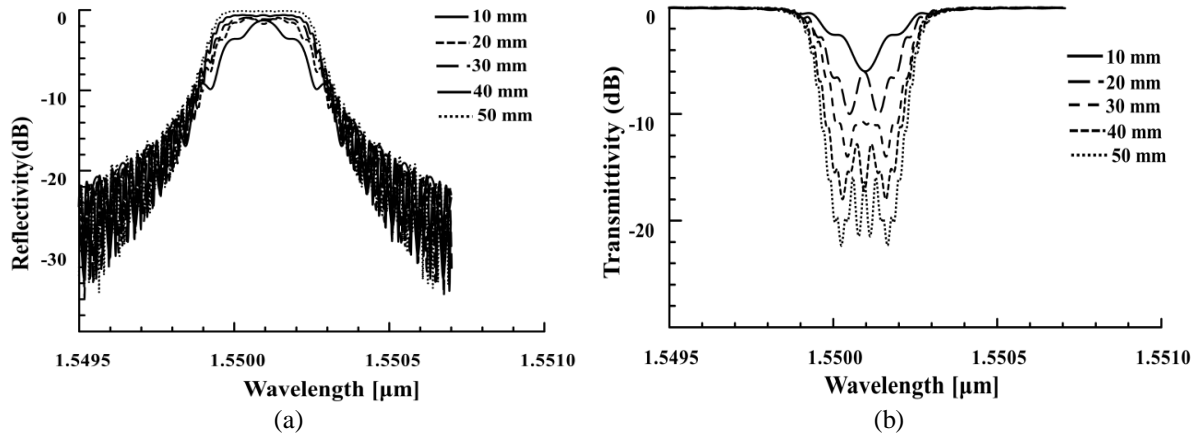


Figure 2. Comparing simulation result in FBG spectrum depend on grating length and temperature 25 °C, (a) reflection and (b) transmission

Table. 2 Spectrum analysis for several grating lengths

Grating length (mm)	FWHM (nm)	SLL (nm)	daya SLL (dB)	SLR (nm)	Power SLR (dB)	Ripple factor	Peak Wavelength (nm)
10	0.4528	1549.714	-13.7218	1550.286	-13.7258	-0.8925	1550
20	0.544	1549.73	-12.5627	1550.27	-12.5654	-0.9651	1550.044
30	0.5376	1549.735	-12.1011	1550.265	-12.1034	-0.987	1550.059
40	0.568	1549.738	-11.8456	1550.262	-11.8496	-0.9952	1549.934
50	0.5552	1549.757	-10.5184	1550.243	-10.5264	-0.998	1549.93

For CFBG with a grating length of 30 nm, the FWHM width is 0.5376, meanwhile SLL and SLR are at 1549.735 nm and 1550.265 nm, the difference between SLL and main-lobe is 0.26 nm, an indication of the difference between SLL and SLR in the large main-lobe, both for sensors [28], [29]. Table 2 also shows that the CFBG experienced a widening of the FWHM along with the increase in the size of the CFBG grating. Meanwhile, the ripple factor also shows a good design as a sensor for a size of 50 mm, so for further analysis, the grating size is used as long as 50 mm. and for Tahn Apodization can be seen in Figure 3. The reflection and transmission spectrum of Tanh Apodization and several Chirped are shown in Figure 3(a) and Figure 3(b) respectively.

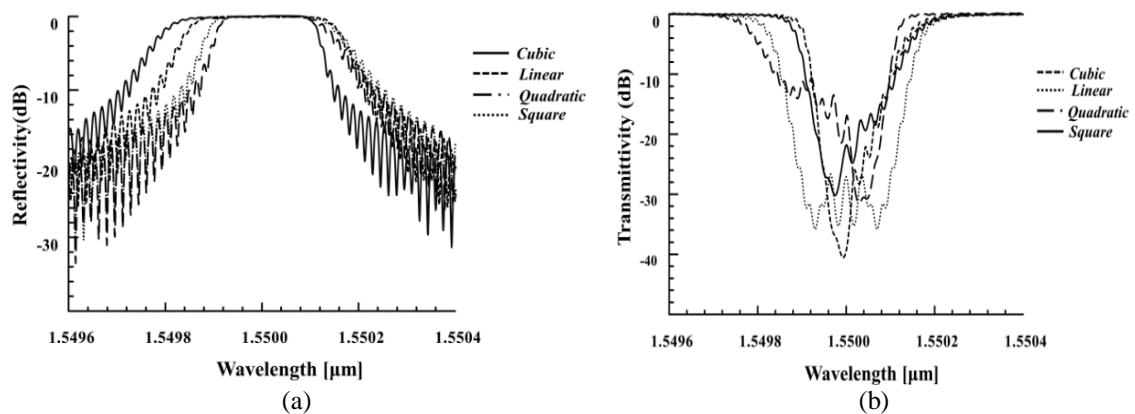


Figure 3. Comparing simulation result FBG with Tanh apodization and several chirped (a) reflection and (b) transmission

Figure 3 shows that the spectrum for Tanh Apodization with several Chirped, from the above spectrum we can obtain the values in the Table 3. As seen in the Figure 3 and Table 3, each value of FWHM, ripple factor and different sidelobe and main-lobe, Tanh Linear CFBG has the narrowest FWHM with a value of 0.5536 nm when compared to other Tanh CFBGs, meanwhile Tanh cubicroot-CFBG has the widest FWHM, FWHM which The width is especially suitable for optical communication applications, to compensate for the dispersion that occurs during data transmission. In terms of ripple factor, Tanh Cubicroot-CFBG has the best ripple factor compared to others. The latter is seen from the different main-lobe and sidelobe. Tanh Cubicroot-CFBG has the largest value, so it is very easy to separate the two lobes. Figure 4 as shown transmission and reflection spectrum varies as function of wavelength as given in Figure 4(a) and Figure 4(b) respectively.

Table 3. Tanh apodization with CFBG type

Chirped	FWHM (nm)	Ripple factor	Different sidelobe and main-lobe
Linear	0.5536	-0.997	0.2432
Quadratic	0.6536	-0.9997	0.1872
Square root	0.6192	-0.9999	0.287
Cubic root	0.6848	0.9999	0.288

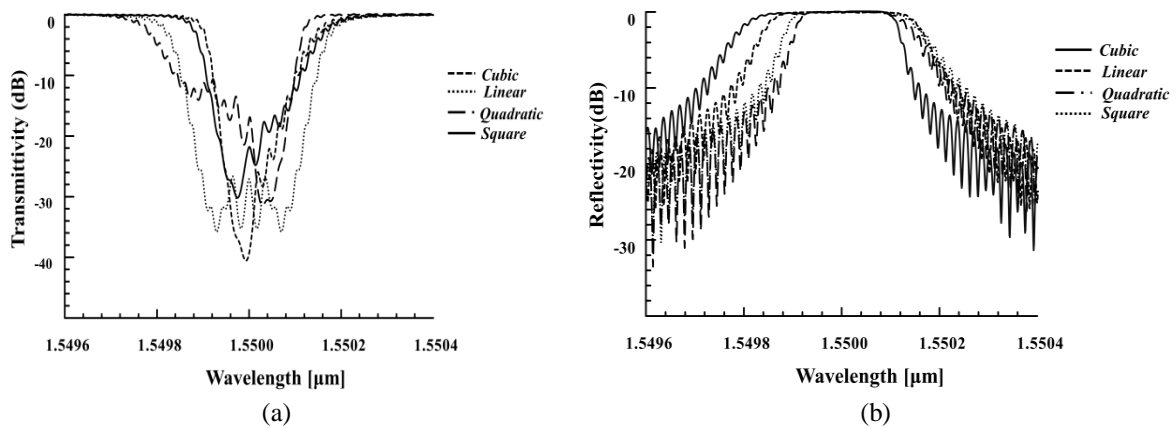


Figure 4. Comparing simulation result FBG with Gaussian apodization and several chirped (a) reflection and (b) transmission

Gaussian apodization can narrow FWHM, following spectrum analysis from Gaussian CFBG, the parameters analysis is given in Table 4. In this section we will look at the FWHM, ripple factor and the different main lobe and sidelobe of the CFBG design, these three factors are very decisive for the performance of the CFBG as a sensor, a large different mainlobe and sidelobe will give a good accuracy of a CFBG sensor, the ripple factor will affect the noise of the resulting spectrum, and A narrow FWHM will clearly show the peak wavelength produced and will give good performance, for further details can be seen in the Table 4.

Table 4. Gaussian apodization with several CFBG

CFBG	FWHM (nm)	Ripple factor	Different main-lobe and sidelobe (nm)
Linear	0.3472	-0.9947	0.372
Quadratic	0.7272	-0.9961	0.33
Square root	0.7352	-0.9981	0.372
Cubic root	0.6664	-0.999	0.388

For each different CFBG, after the simulation, spectrum data is obtained as in the Table 4, which is devoted to Gaussian apodization, it was found that Gaussian linear-CFBG obtained a narrow FWHM compared to other types of CFBG, and this will be recommended for application as a sensor because it requires a spectrum with a narrow FWHM. Meanwhile, what is interesting from the results above is that Gaussian Cubicroot-CFBG has a good ripple factor compared to other gaussian CFBGs, this is good for

sensor application and dispersion compensation. Meanwhile, when viewed from the different main-lobe and sidelobe, the Gaussian Cubicroot-CFBG has the farthest difference compared to other gaussian CFBGs. In dispersion communication, FBG is needed which can reduce signal reflection. Meanwhile, for FBG as a sensor, an FBG with a narrow FWHM is needed and is able to easily distinguish the peak lobe from the side lobe. Figure 5 shows the Gaussian linear-CFBG reflection and transmission spectrum shifts with temperature changes in the range of 25 °C to 105 °C.

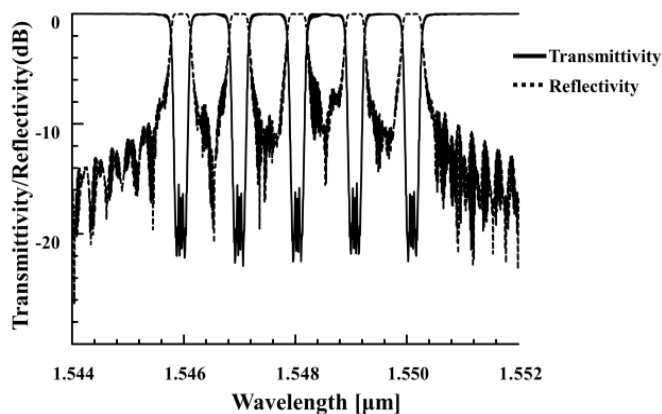


Figure 5. Bragg wavelength shift with a change in temperature

As shown in the (7), the shift of each spectrum is obtained, setup thermal expansion and thermo-optic coefficient as TOPAS material. In the shift wavelength, it was found that for every 1 °C temperature change, the Bragg wavelength shift is -51.63 pm for Gaussian linear-CFBG, with the coefficient of thermal expansion given in the Table 1. The Bragg wavelength shifts to the left from the 1550 nm wavelength. This is caused by the coefficient of negative thermal expansion as shown in the Table 1. It can be seen in Figure 5 that the red line shows the transmission spectrum and the blue line shows the reflection spectrum of CFBG with total chirp of 0.1 nm. This result is much larger than previously reported for uniform FBG with the same material. This result also shows a greater sensitivity of CFBG with TOPAS material compared to silica material which produces a sensitivity of ~14 pm/°C [29]. The sensitivity CFBG with Gaussian and Tanh apodization and other chirped as Table 5.

Table 5. The sensitivity apodization with CFBG type

Apodization	Chirpe	Sensitivity (pm/°C)
Gaussian	Linear	-51.63
Gaussian	Quadratic	-51.75
Gaussian	Square root	-51.63
Gaussian	Cubic root	-51.74
Tanh	Linear	-51.76
Tanh	Quadratic	-51.61
Tanh	Square root	-51.74
Tanh	Cubic root	-51.73

Table 5 shows how the effect of chirped and apodization on the sensitivity of FBG, CFBG produces a wide reflection wave peak, so it has a peak with a wide range, Tanh linear-CFBG has a sensitivity of -51.76 pm/°C and only has a slight difference when compared to apodization and chirped. another type, for gaussian apodization, Gaussian quadratic-CFBG has the highest sensitivity of -51.75 pm/°C with only a slight difference in sensitivity. so that the accuracy of the sensor is also needed when viewed from the reflection spectrum.

5. CONCLUSION

CFBG has been designed with TOPAS material, it was found that CFBG can be applied in optical sensors for temperature, performance factors such as sensitivity, ripple factor, SLR, SLL and different mainlobe and sidelobe were investigated and found that the TOPAS Tanh Linear-CFBG sensitivity was -

51.76 pm/°C, this result is much greater when compared to Uniform FBG TOPAS. When viewed in terms of accuracy, cubicroot provides good accuracy, this can be seen from the large difference in the main lobe and side lobe. this applies to both apodizations, with values of 0.288 nm for Tanh and 0.388 nm for Gaussian.

ACKNOWLEDGEMENTS

We would like to thank LPPM University of Riau for their great support in this research. We also would like to thank physics education laboratory and plasma and photonics physics laboratory.




REFERENCES

- [1] T. Saktioto, K. Ramadhan, Y. Soerbakti, D. Irawan, and Okfalisa, "Integration of chirping and apodization of Topas materials for improving the performance of fiber Bragg grating sensors," *Journal of Physics: Conference Series*, vol. 2049, no. 1, p. 012001, Oct. 2021, doi: 10.1088/1742-6596/2049/1/012001.
- [2] Q. Wang, L. Zhang, C. Sun, and Q. Yu, "Multiplexed fiber-optic pressure and temperature sensor system for down-hole measurement," *IEEE Sensors Journal*, vol. 8, no. 11, pp. 1879–1883, Nov. 2008, doi: 10.1109/JSEN.2008.2006253.
- [3] S. Goossens *et al.*, "A global assessment of barely visible impact damage for CFRP sub-components with FBG-based sensors," *Composite Structures*, vol. 272, p. 114025, Sep. 2021, doi: 10.1016/j.compstruct.2021.114025.
- [4] D. Tosi *et al.*, "Fiber-optic chirped FBG for distributed thermal monitoring of ex-vivo radiofrequency ablation of liver," *Biomedical Optics Express*, vol. 5, no. 6, p. 1799, Jun. 2014, doi: 10.1364/boe.5.001799.
- [5] J. Juraszek, M. Gwóźdź-Iasoń, and D. Logoń, "Fbg strain monitoring of a road structure reinforced with a geosynthetic mattress in cases of subsoil deformation in mining activity areas," *Materials*, vol. 14, no. 7, p. 1709, Mar. 2021, doi: 10.3390/ma14071709.
- [6] M. M. A. Eid, A. S. Seliem, A. N. Z. Rashed, A. E. N. A. Mohammed, M. Y. Ali, and S. S. Abaza, "High sensitivity sapphire FBG temperature sensors for the signal processing of data communications technology," *Indonesian Journal of Electrical Engineering and Computer Science*, vol. 21, no. 3, pp. 1567–1574, Mar. 2021, doi: 10.11591/ijeecs.v21.i3.pp1567-1574.
- [7] B. Zhang and M. Kahrizi, "High-temperature resistance Fiber Bragg grating temperature sensor fabrication," *IEEE Sensors Journal*, vol. 7, no. 4, pp. 586–591, Apr. 2007, doi: 10.1109/JSEN.2007.891941.
- [8] A. I. Gusarov, "Temperature monitoring of nuclear reactor cores with multiplexed fiber Bragg grating sensors," *Optical Engineering*, vol. 41, no. 6, p. 1246, Jun. 2002, doi: 10.1117/1.1475739.
- [9] K. Dey, N. Vangety, and S. Roy, "Machine learning approach for simultaneous measurement of strain and temperature using FBG sensor," *Sensors and Actuators A: Physical*, vol. 333, p. 113254, Jan. 2022, doi: 10.1016/j.sna.2021.113254.
- [10] M. Mansoursamaei and A. Malakzadeh, "Simultaneous measurement of temperature and strain using a single fiber bragg grating on a tilted cantilever beam," *Optical Review*, vol. 28, no. 3, pp. 289–294, Jun. 2021, doi: 10.1007/s10043-021-00660-w.
- [11] P. M. Cavaleiro, F. M. Araújo, L. A. Ferreira, J. L. Santos, and F. Farahi, "Simultaneous measurement of strain and temperature using Bragg gratings written in germanosilicate and boron-codoped germanosilicate fibers," *IEEE Photonics Technology Letters*, vol. 11, no. 12, pp. 1635–1637, Dec. 1999, doi: 10.1109/68.806871.
- [12] A. Othonos, K. Kalli, and G. E. Kohnke, "Fiber Bragg gratings: Fundamentals and applications in telecommunications and sensing," *Physics Today*, vol. 53, no. 5, pp. 61–62, May 2000, doi: 10.1063/1.883086.
- [13] K. Markowski, K. Jędrzejewski, M. Marzęcki, and T. Osuch, "Linearly chirped tapered fiber-Bragg-grating-based Fabry-Perot cavity and its application in simultaneous strain and temperature measurement," *Optics Letters*, vol. 42, no. 7, p. 1464, Apr. 2017, doi: 10.1364/ol.42.001464.
- [14] C. A. F. Marques, P. Antunes, P. Mergo, D. J. Webb, and P. Andre, "Chirped Bragg gratings in PMMA step-index polymer optical fiber," *IEEE Photonics Technology Letters*, vol. 29, no. 6, pp. 500–503, Mar. 2017, doi: 10.1109/LPT.2017.2662219.
- [15] R. L. Rito, S. L. Ogin, and A. D. Crocombe, "An experimental and numerical study on the use of chirped fbg sensors for monitoring fatigue damage in hybrid composite patch repairs," *Sensors (Switzerland)*, vol. 21, no. 4, pp. 1–17, Feb. 2021, doi: 10.3390/s21041168.
- [16] Y. Barbarin *et al.*, "Development of a shock and detonation velocity measurement system using chirped fiber bragg gratings," *Sensors (Switzerland)*, vol. 20, no. 4, p. 1026, Feb. 2020, doi: 10.3390/s20041026.
- [17] J. Pooley, E. Price, J. W. Ferguson, and M. Ibsen, "Optimised chirped fibre bragg gratings for detonation velocity measurements," *Sensors (Switzerland)*, vol. 19, no. 15, p. 3333, Jul. 2019, doi: 10.3390/s19153333.
- [18] G. Palumbo, D. Tosi, A. Iadicco, and S. Campopiano, "Analysis and design of chirped fiber Bragg grating for temperature sensing for possible biomedical applications," *IEEE Photonics Journal*, vol. 10, no. 3, pp. 1–15, Jun. 2018, doi: 10.1109/JPHOT.2018.2829623.
- [19] S. Korganbayev *et al.*, "Detection of thermal gradients through fiber-optic chirped fiber Bragg grating (CFBG): Medical thermal ablation scenario," *Optical Fiber Technology*, vol. 41, pp. 48–55, Mar. 2018, doi: 10.1016/j.yofte.2017.12.017.
- [20] A. F. Sayed, F. M. Mustafa, A. A. M. Khalaf, and M. H. Aly, "Spectral width reduction using apodized cascaded fiber Bragg grating for post-dispersion compensation in WDM optical networks," *Photonic Network Communications*, vol. 41, no. 3, pp. 231–241, Jun. 2021, doi: 10.1007/s11107-021-00926-y.
- [21] B. Gul and F. Ahmad, "Comparative performance analysis of Tanh-apodized fiber Bragg grating and Gaussian-apodized fiber Bragg grating as hybrid dispersion compensation model," in *Lecture Notes in Networks and Systems*, vol. 244, 2022, pp. 71–82.
- [22] A. F. Sayed, T. M. Barakat, and I. A. Ali, "A novel dispersion compensation model using an efficient CFBG reflectors for WDM optical networks," *International Journal of Microwave and Optical Technology*, vol. 12, no. 3, pp. 230–238, 2017.
- [23] J. X. Cai, K. M. Feng, A. E. Willner, V. Grubsky, D. S. Starodubov, and J. Feinberg, "Simultaneous tunable dispersion compensation of many WDM channels using a sampled nonlinearly chirped fiber Bragg grating," *IEEE Photonics Technology Letters*, vol. 11, no. 11, pp. 1455–1457, Nov. 1999, doi: 10.1109/68.803077.
- [24] D. Meena and M. L. Meena, "Design and analysis of novel dispersion compensating model with chirp fiber bragg grating for long-haul transmission system," in *Lecture Notes in Electrical Engineering*, vol. 546, 2020, pp. 29–36.
- [25] P. Bettini, E. Guerreschi, and G. Sala, "Development and experimental validation of a numerical tool for structural health and usage monitoring systems based on chirped grating sensors," *Sensors (Switzerland)*, vol. 15, no. 1, pp. 1321–1341, Jan. 2015, doi: 10.3390/s150101321.




- [26] A. Nand et al., "Determination of the position of a localized heat source within a chirped fibre Bragg grating using a Fourier transform technique," *Measurement Science and Technology*, vol. 17, no. 6, pp. 1436–1445, Jun. 2006, doi: 10.1088/0957-0233/17/6/023.
- [27] U. K. Uma, D. Samiappan, K. R., and T. Sudhakar, "Development and experimental validation of a nuttall apodized fiber Bragg grating sensor with a hydrophobic polymer coating suitable for monitoring sea surface temperature," *Optical Fiber Technology*, vol. 56, p. 102176, May 2020, doi: 10.1016/j.yofte.2020.102176.
- [28] T. Saktioto, K. Ramadhan, Y. Soerbakti, R. F. Syahputra, D. Irawan, and Okfalisa, "Apodization sensor performance for TOPAS fiber Bragg grating," *Telkomnika (Telecommunication Computing Electronics and Control)*, vol. 19, no. 6, pp. 1982–1991, Dec. 2021, doi: 10.12928/TELKOMNIKA.v19i6.21669.
- [29] H. M. El-Gammal, E. S. A. El-Badawy, M. R. M. Rizk, and M. H. Aly, "A new hybrid FBG with a π -shift for temperature sensing in overhead high voltage transmission lines," *Optical and Quantum Electronics*, vol. 52, no. 1, p. 53, Jan. 2020, doi: 10.1007/s11082-019-2171-7.

BIOGRAPHIES OF AUTHORS






Dr. Dedi Irawan, M. Sc    is a lecturer at Physics Education, Dept. of Education of Mathematics and Natural Sciences, Universitas Riau, Pekanbaru, Indonesia. He works on basic and advanced Photonics. He has published many articles and supervised Master degree and Doctoral degree since 2015 in Universiti Teknologi Malaysia. Currently research focus in Fiber Bragg Grating sensor (FBG), Mach-zehnder Interferometer. Furthermore, he is also doing some research in optoelectronic and optical sensor utilizing FBG, MZI, and directional coupler for medical and agricultural application. He can be contacted at email: dedi.irawan@lecturer.unri.ac.id.






Khaikal Ramadhan S. Si    was a student at the University of Riau in 2017 and has finished studying Physics at the University of Riau with a B.Sc degree in 2021. He interests include applied physics, Photonics, Optical Fiber for communication and sensor. currently joint research focus in Fiber bragg grating sensor, MZI, PCF-SPR. He can be contacted at email: khaikal.ramadhan4946@student.unri.ac.id.



Prof. Dr. Saktioto, S. Si., M. Phil    is a Senior lecturer at Physics Dept., Faculty of Mathematics and Natural Sciences, Universitas Riau, Pekanbaru, Indonesia. He works on Plasma and Photonics Physics. He has published numbers of article in indexed journal reporting his work in plasma photonic, and it's related with fiber coupler fabrication. He also active doing supervision in Master and Doctoral degree since 2009. Currently his research focus is photonics and plasma industry for communication and biosensors. He can be contacted at email: Saktioto@yahoo.com.



Azwir Marwin    was a student at the University of Riau in 2019. His interests include applied physics, pure physics. Now he works on optoelectronics laboratory as laboratory assistant. And also joint with research focus in Fiber bragg grating sensor, Mach-zehnder interferometer. He can contacted at email: azwir.marwin4971@student.unri.ac.id.